ISSN 0023-1584, Kinetics and Catalysis, 2007, Vol. 48, No. 3, pp. 367–375. © MAIK "Nauka/Interperiodica" (Russia), 2007.
Original Russian Text © O.V. Skrebkov, S.P. Karkach, 2007, published in Kinetika i Kataliz, 2007, Vol. 48, No. 3, pp. 388–396.

Vibrational Nonequilibrium and Electronic Excitation in the Reaction of Hydrogen with Oxygen behind a Shock Wave

O. V. Skrebkov and S. P. Karkach

Institute of Problems of Chemical Physics, Russian Academy of Sciences, Chernogolovka, Moscow oblast, 142432 Russia
E-mail: skreb@icp.ac.ru

Received February 28, 2006

Abstract—A theoretical analysis of ignition and combustion processes in a hydrogen–oxygen mixture behind a shock wave is presented (1000 K ≤ T ≤ 2500 K; 2.0 atm ≥ P ≥ 0.3 atm). The experiments performed using stoichiometric mixtures with the detection of OH ($^2\Sigma^+$) and rich mixtures with the detection of OH ($^2\Pi$) were interpreted in terms of a general kinetic approach. In this case, the apparent rate constant of the chain branching reaction H + O_2 ⟶ O + OH was the only adjustable parameter. It was found that this rate constant increased with decreasing hydrogen content and exceeded equilibrium values. In this context, the mechanism of chain branching, which occurs through the formation of the vibrationally excited radical $HO_2(v)$, and the role of secondary vibrationally nonequilibrium O_2 and $O_2(^1\Delta)$ molecules and the reaction H + $O_2(^1\Delta)$ ⟶ O + OH are discussed. New mechanisms of the formation and quenching of electronically excited OH($^2\Sigma^+$) radicals, O(^1D) atoms, and $O_2(^1\Delta)$ molecules are considered. The results of a nonempirical (ab initio) analysis of molecular systems and the corresponding estimations of reaction rate constants were widely used.

DOI: 10.1134/S0023158407030044

INTRODUCTION

A hydrogen–oxygen reacting mixture, which is most important from the practical standpoint, remains over decades a central model system containing all of the key details of the kinetics of gas-phase ignition, combustion, and detonation processes (see [1–23] and references therein). The $H_2 + O_2$ system has been studied by the shock tube method (e.g., see review [10]). The experimental results obtained by this method are particularly convenient for comparing with kinetic calculations. Thus, the effect of walls is negligibly small under appropriately chosen conditions; the self-heating of a mixture can be ignored at low concentrations of a reacting additive (for more detail, see [22]); and a single reaction can be practically considered at a minimum of parameters and assumptions with a specially chosen composition of the mixture (e.g., see [20]).

Nevertheless, as a rule, the rate constants of the most important reactions determined by different authors even in the purest experiments differed by a factor of 2–3 or higher. A reason for this is that overall reactions were taken into account along with elementary reactions in these calculations. In this context, nonempirical sources of kinetic information become of particular importance. However, the most important reason for the above differences is the neglect of the effect of vibrational nonequilibrium and electronic excitation, which naturally appear in the course of combustion and differently manifest themselves at various stages of an experiment depending on the composition of the mixture. This problem is considered below as applied to the most important chain branching reaction H + O_2 ⟶ O + OH.

The following concentrations of the most important components are characteristic of experiments in shock tubes and compositions with an insignificant concentration of a reacting additive, less than 5% ($2H_2 + O_2$) [22, 23], mol/cm^3: H_2, O_2, and H_2O ~ 10^{-7}; H, O, and OH (OH($^2\Pi$)) ~ 10^{-8}–10^{-9}; HO_2 and $O_2^*(O_2(^1\Delta))$ ~ 10^{-9}–10^{-10}; HOOH, ~ 10^{-11}; O*(O(^1D)) ~ 10^{-12}; OH*(OH($^2\Sigma^+$)) ~ 10^{-15}–10^{-17}. Although the concentrations of OH* radicals are low, their emission

$$OH^* \longrightarrow OH, \quad h\nu \approx 47\,000 \text{ K } (\lambda \approx 306 \text{ nm})$$

has long been used in research practice to determine the induction time of ignition. Belles and Lauver [4] considered the main features of the overall kinetics of formation of the OH* radical; the question of the detailed mechanism of OH* formation is still an open question (see Section 4). In this case, the role of electronically excited O* and O_2^* species, which have lower excitation energies,

$$O \longrightarrow O^*, \quad h\nu \approx 22\,800 \text{ K};$$
$$O_2 \longrightarrow O_2^*, \quad h\nu \approx 11\,400 \text{ K}$$

is unclear.

The importance of answers to these questions is directly related to the search for effective means of affecting ignition and combustion processes.

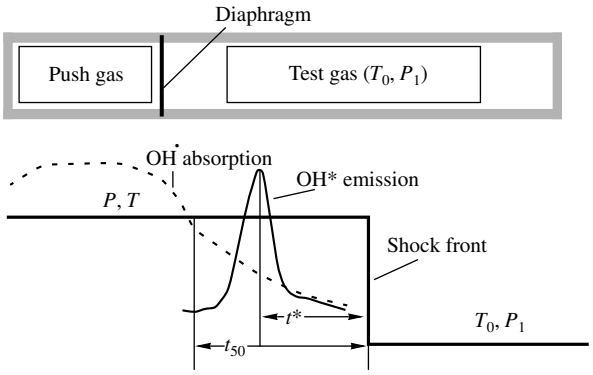

Fig. 1. Schematic diagram of shock tube experiments. Measured values: t^* is the time between a shock front and the point in time at which the emission OH* ⟶ OH reached a maximum; t_{50} is the time between a front and the point in time at which the light absorption OH ⟶ OH* reached a half of its maximum value.

EXPERIMENTAL

Previously [22], the electronically excited OH* radical was detected behind an incident shock wave using emission spectroscopy. The stoichiometric mixtures of $2H_2 + O_2$ diluted with argon were studied; the time t^* (Fig. 1) between a shock front and the point in time at which emission at $\lambda = 306$ nm reached a maximum (in the calculations, it was identified with the point in time at which a maximum concentration of OH* was reached) was measured.

In this work, we also employed experimental results obtained by Ryu et al. [16] using another technique under different conditions: a reflected shock wave, the detection of the OH radical in the ground electronic state by absorption spectroscopy, rich mixtures of $H_2 + O_2 + Ar$, and the time between a front and the point in time at which light absorption by the OH radical reached a half of its maximum value (t_{50}, see Fig. 1; in the calculations, the point in time at which a half-maximum concentration of OH radicals was reached).

The published experimental results [16, 22] were chosen because they are best suited for a direct comparison with the results of isothermal kinetic calculations (a small impurity of a reacting mixture in an inert gas and, consequently, a minimized heat effect of exothermic reactions on gas dynamics; for more detail, see [22]).

THEORETICAL

The nonempirical (ab initio) analysis of a number of molecular systems was performed in order to distinguish the elementary steps of reactions and independently evaluate the equilibrium rate constants. Quantum-chemical calculation programs from the GAUSSIAN [24] and GAMESS [25] software packages were used in combination with a previously proposed procedure [26] for predicting the energy of a molecular system at the stationary points of a potential energy surface by a special treatment of a series of calculations. The following statistical methods were used for evaluating rate constants: conventional transition state theory (CTST) and variational transition state theory (VTST). The degradation of highly excited complexes $\{H\cdots O_2\} = HO_2(v)$ and $\{HO_2\cdots H\}=HOOH(v) \longleftrightarrow H_2OO(v)$ was analyzed in terms of the Landau statistical theory (LST) (e.g., see [27]). The required parameters of theory were taken from ab initio calculations and compared with the results of trajectory calculations (dynamic reaction coordinate (DRC) option from the GAMESS package [25]) on the same potential energy surfaces of the systems. The ab initio calculations are considered in detail in the text.

The general formulation of the problem of the calculation of a chemically and vibrationally nonequilibrium flow of a multicomponent gas mixture was considered previously [28, 29]. In this work, vibrational nonequilibrium was systematically taken into account only for starting (primary) molecules of H_2 and O_2. We intend to consider nonequilibrium effects in more detail later on. Here, the problem is simplified to an isothermal problem: we believe that the mixture of $H_2 + O_2$ is strongly diluted with an inert gas so that the heat effects of reactions can be ignored. Under these conditions, it is sufficient to integrate two Landau–Teller equations. As a result, we obtain analytic functions for the vibrational temperatures of H_2 and O_2:

$$E_k(t) = E_k^0 - [E_k^0 - E_k(0)]\exp(-t/\tau_{vib}),$$
$$T_k(t) = \theta_k/\ln\{[1 + E_k(t)]/E_k(t)\},$$

where E_k and T_k are the vibrational energy and temperature of the kth mode (in our case, H_2 or O_2) and E_k^0 and $E_k(0)$ are the equilibrium and initial values of $E_k(t)$. The effect of vibrational nonequilibrium on the rates of chemical reactions was calculated in terms of a model [28, 29] using the equations

$$k(T, T_k) = \kappa_r(T, T_k)k_r^0(T),$$

$$\kappa_r(T, T_k) = \exp\left[E_r\left(\frac{1}{T} - \frac{\sum_i \beta_{ri}^2}{\sum_i \beta_{ri}^2 T_i}\right)\right], \quad (1)$$

$$E_r = \begin{cases} E_r^A - (\xi_r + 4)T/2 \\ 0, \quad E_r \le 0. \end{cases} \quad (2)$$

Here, $k_r^0(T)$ is the equilibrium rate constant of the rth reaction; E_r^A is the activation energy of the rth reaction; E_r is the fraction of the activation energy of the rth reaction that accounts for the vibrational degrees of freedom of reactant molecules (obtained by subtracting

rotational and translational energies from the activation energy); ξ_r is the number of the rotational degrees of freedom of the molecules; and β_{ri} are the expansion coefficients of the rth reaction coordinate in normal vibrations (modes).

At comparatively high temperatures ($T > 1400$ K), the effect of the vibrational relaxation of the parent molecules of H_2 and O_2 manifested itself in the inhibition of the initiation reaction with the participation of these molecules. The effect of vibrational nonequilibrium increases with temperature and activation energy because the Landau–Teller temperature dependence of vibrational relaxation time is weaker than the Arrhenius dependence of k_r^0. Thus, at a high temperature, vibrational equilibrium with respect to oxygen has no time to be established before the end of the induction period and the multiplier $\kappa_r(T, T_k)$ in Eq. (1) is much lower than 1 over a small time interval of the initial step of initiation (see Fig. 2). The integrated effect resulted in an increase in the induction period.

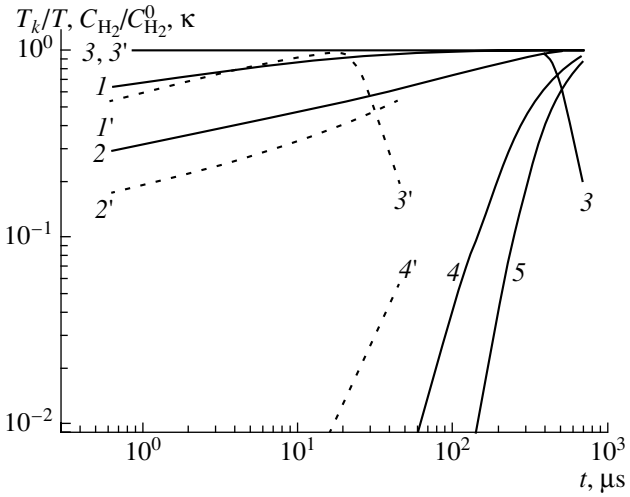

Fig. 2. Calculated profiles of vibrational temperatures (*1*, *1'*) T_{H_2} and (*2*, *2'*) T_{O_2} related to equilibrium values; (*3*, *3'*) H_2 concentration related to the initial value; and (*4*, *4'*, *5*) the values of κ_1 and κ_2 for initiation reactions (1) and (2) (see the table); (*1*–*5*) calculation at $T = 1100$ and $P = 1.96$ atm; (*1'*–*4'*) calculation at $T = 2300$ and $P = 0.5$ atm (in this case, $\kappa_2 < 10^{-2}$). Starting H_2/O_2/Ar mixture: 1.8 : 0.9 : 97.3.

RESULTS AND DISCUSSION

To describe the above experiments, we used a kinetic scheme that involved reactions with the participation of H_2, O_2, H_2O, $HO_2^{\cdot}$, H, OH, O, H_2O_2, O_3, O_2^*, O*, and OH*. The table summarizes the main reactions responsible for the mechanism of chemical transformations in general, as well as the mechanism of formation and quenching of OH* radicals. The accepted values of equilibrium rate constants $k_r^0(T)$ were chosen based on published data [30, 31] (with consideration for the temperature range), results [16, 20, 32–34], and our estimations based on an ab initio analysis, as well as by fitting calculated values to experimental data. The molecular constants and thermodynamic characteristics were consistent with reference data [35, 36].

1. Mechanism of Initiation

In the kinetic calculations performed in this work, in addition to reactions (1) and (2) and reverse reactions (28') and (29') from the table, the following bimolecular initiation processes were taken into account in the full kinetic scheme:

$$\text{(i3)}\ H_2 + O_2 \longleftrightarrow H_2O + O,$$

$$k_{i3}^0 < 2 \times 10^{12}(T/298)^{1.8}\exp(-34000/T)\ \text{(CTST)},$$

$$\text{(i4)}\ H_2 + O_2 \longleftrightarrow 2OH,$$

$$k_{i4}^0 < 3 \times 10^{12}(T/298)^{1.9}\exp(-34400/T)\ \text{(CTST)},$$

$$\text{(i5)}\ O_2 + M \longleftrightarrow 2O + M,$$

$$k_{i5}^0 = 3 \times 10^{14}\exp(-58410/T)\ [31].$$

The trimolecular reactions

$$\text{(i6)}\ H_2 + 2O_2 \longrightarrow H + \{HO_2\cdots O_2\},$$

$$HOOH + O_2/O_2^*, 2HO_2$$

with the overall rate constant

$$k_{i6}^0 \approx 0.7 \times 10^3(T/298)k_1^0\exp(\Delta E^A/T),\ \Delta E^A \approx 3000\ \text{K}, \quad (3)$$

were also taken into account. In this case, the first process of (i6) can occur on the potential energy surfaces of the H_2O_4 system at all of the allowed multiplicities of 1, 3, and 5.

Initiation depends on bimolecular reaction (1) over wide temperature and pressure ranges. In the regions of high temperatures ($T > 2200$ K) and low pressures ($P < 0.6$ atm), reaction (2) becomes significant; reaction (i5) has an effect only with the use of lean mixtures [20]. Michael et al. [20] estimated the apparent rate constant of reaction (1) $k_1 = 7.7 \times 10^{11}(T/298)^{2.433}\exp(-26926/T)$ at $T = 1662$–2097 K; this estimated value is 0.7–0.8 of the theoretically estimated value of k_1^0 given in the table. Recall that, at the step of initiation ($T_k < T$ for the initial molecules of O_2 and H_2), the value of $k_1(T, T_k)$ is lower than the equilibrium value $k_1^0(T)$ (see Theoretical and Fig. 2). Based on the average value of published data [31], $k_1 = 3.9 \times 10^{12}(T/298)^{1.204}\exp(-28230/T)$ is noticeably smaller. We explain the above by the fact that, in the interpretation of experiments, other authors took into account the overall processes $H_2 + O_2 \longrightarrow H_2O + O$, 2OH in addition to reaction (1) (see the estimations of corresponding apparent rate constants in

Reactions and their equilibrium rate constants $k_r^0 = A_r(T/298.15)^n \exp(-E_r^A/T)$ ($cm^3\ mol^{-1}\ s^{-1}$) in a mixture of $H_2 + O_2 + Ar$ at 1000 K ≤ T ≤ 2500 K, 2.0 atm ≥ P ≥ 0.3 atm used in calculations in the interpretation of experimental data [16, 22, 23]

r	Reactions	M	A_r	n	E_r^A	Notes
			Initiation			
1	$H_2 + O_2 \longleftrightarrow H + HO_2$	–	2.2×10^{12}	2.056	27059	[a]
2	$H_2 + M \longleftrightarrow 2H + M$	H_2	9.0×10^{14}	–	48350	[31]
		Ar	2.0×10^{14}	–	48350	
			Chain branching, chain propagation, and other reactions			
3	$HO + H_2 \longleftrightarrow H_2O + H$	–	1.1×10^{12}	1.779	1558	[a]
4	$H + O_2 \longleftrightarrow HO + O$	–	1.2×10^{14}	0.250	8200	[b]
5	$H_2 + O \longleftrightarrow H + HO$	–	1.1×10^{13}	0.861	4648	[a]
6	$HO_2 + H_2 \longleftrightarrow HOOH + H$	–	2.6×10^{12}	–	10750	[31]
7	$H + O_2 + M \longleftrightarrow HO_2 + M$	H_2, O_2	2.0×10^{16}	–0.800	–	[31]
		Ar	7.0×10^{15}	–0.800	–	
8	$O_2 + O + M \longleftrightarrow O_3 + M$	H_2, O_2	9.1×10^{13}	–1.300	–	[31]
		Ar	4.9×10^{13}	–1.000	–	
9	$HO_2 + H \longleftrightarrow HO + OH$	–	3.8×10^{13}	0.486	103	[31]
10	$O + HO_2 \longleftrightarrow OH + O_2$	–	1.5×10^{13}	0.330	–128	[31]
11	$HO + HO \longleftrightarrow H_2O + O$	–	2.1×10^{10}	2.700	–1251	[16]
12	$H + OH + M \longleftrightarrow H_2O + M$	H_2	1.3×10^{17}	–1.212	–295	[31]
		O_2	3.1×10^{16}	–1.212	–295	
		Ar	9.4×10^{16}	–2.000	–	
13	$H_2O_2 + M \longleftrightarrow HO + OH + M$	–	3.2×10^{17}	–	23820	[31]
14	$OH + HO_2 \longleftrightarrow H_2O + O_2$	–	3.1×10^{13}	–	73	[31]
15	$2HO_2 \longleftrightarrow H_2O_2 + O_2$	–	1.3×10^{12}	–	–67	[31]
			Electronic excitation and quenching of OH*, O*, and O_2^*			
16	$HO_2 + H_2 \longleftrightarrow OH^* + H_2O$	–	$<6.0 \times 10^{14}$	–0.300	21700	[c]
17	$O^* + H + M \longleftrightarrow OH^* + M$	–	5.0×10^{15}	–1.000	–	[c]
18	$O + H + M \longleftrightarrow OH^* + M$	H_2, O_2, Ar	1.0×10^{16}	–1.000	12000	[c]
		OH	2.0×10^{15}	–1.000	–	
19	$OH^* + M \longleftrightarrow OH + M$	H_2O	2.2×10^{14}	–	276	[32, 33][c]
		O_2	6.0×10^{12}	–	–	
		H_2	1.0×10^{12}	–	–	
		Ar	1.3×10^{11}	0.500	–	
20	$OH^* + O_2 \longleftrightarrow O_3 + H$	–	4.0×10^{13}	0.500	–	[32, 33][c]
21	$OH^* + H_2O \longleftrightarrow H_2O_2 + H$	–	7.5×10^{12}	–	276	[32, 33][c]
22	$OH^* + H_2 \longleftrightarrow H_2O + H$	–	8.8×10^{13}	0.500	–	[32, 33][c]
23	$OH^* + O_2 \longleftrightarrow HO_2 + O$	–	2.0×10^{13}	0.500	–	[32, 33][c]
24	$OH^* \longleftrightarrow OH + h\nu$	–	1.4×10^{6}	–	–	[34]
25	$HO_2 + H \longleftrightarrow H_2O + O^*$	–	2.3×10^{13}	0.458	678	[31][d]
26	$O^* + H_2 \longleftrightarrow OH + H$	–	8.7×10^{13}	–	–14	[31]
27	$O^* + M \longleftrightarrow O + M$	H_2	1.0×10^{14}	–	–	[31]
		O_2, Ar	2.0×10^{11}	–	–	
28	$H + HO_2 \longleftrightarrow H_2 + O_2^*$	–	6.5×10^{11}	1.671	3162	[a]
29	$O_2^* + M \longleftrightarrow O_2 + M$	H_2, O_2	$\approx 2.0 \times 10^{6}$	–	–	[31]
		Ar	$\leq 1.0 \times 10^{5}$	–	–	

[a] CTST estimation.
[b] Average effective value in fitting calculated values to experimental data (see the text and Fig. 8).
[c] The result of fitting calculated values to experimental data (see the text).
[d] LST and DRC estimations (see the text).

[8, 20]). Recall that, of the processes $H_2 + O_2 \longrightarrow H + HO_2$, $H_2O + O$, and 2OH, only the first is an elementary reaction, which is consistent with the rule of conservation of molecular symmetry in thermal single-step reactions (see [20, 37]). Bimolecular reactions (i3) and (i4) are every bit as possible as the formation of the intermediate complex $\{H\cdots HO_2\}$, that is, by an indirect mechanism, and they have high activation energies [26, 37]. Note that previous calculations [38, 39] with the use of LEPS and the many-body expansion (MBE) potentials many times overestimated the rate constants of processes (i3) and (i4) because of the presence of nonphysical gaps in the above potential energy surfaces.

In the absence of external sources of O_2^*, the contribution of reactions (29') and (28') to initiation is negligibly small because of the low rate of electronic relaxation (29') on heating the mixture, $k^0_{29'} \sim 10^6 \times \exp(-11400/T)$.

The above rate constant of trimolecular reactions (i6) is based on the ab initio evaluation of the statistical characteristics of transition states in reaction (i6) and a decrease of the threshold by the bonding energy of the $\{HO_2\cdots O_2\}$ complex ΔE^A. Previously [23], we estimated $k_{i6} \approx 2 \times 10^{17}\exp(-13000/T)$ based on available experimental data on the rate constant of the reverse reaction $2HO_2 \longrightarrow H_2 + 2O_2$ (see [31]); now, this value seems overestimated ($\Delta E^A \approx 14000$ K in item (3) above). It is likely that the above experimental data were obtained with the participation of vibrationally excited radicals $HO_2(v)$ (see the discussion of the rate of the reaction $H + HO_2(v) \longrightarrow H_2 + O_2^*$ in Section 3).

In accordance with the above estimations, the ratio between the rates of bimolecular and trimolecular initiation is

$$W^0_{i6}/W^0_1 = 0.7 \times 10^3 (T/298)\exp(3000/T)\, C_{O_2}$$

$$= 3 \times 10^{-2}\exp(3000/T)\, P_{O_2}$$

(here, C_{O_2} is expressed in mol/cm^3 and P_{O_2}, in atm). Thus, at 1000 K, bimolecular initiation is predominant up to the partial pressure of oxygen $P_{O_2} \approx 1.5$ atm.

Note that the mechanism of initiation in the hydrogen–oxygen system at low temperatures and high pressures remains unclear and calls for special investigations, both experimental and theoretical.

2. Chain Branching and Propagation

The reaction $H + O_2 \longrightarrow HO + O$ (see reaction (4) in the table) does not practically occur by a direct mechanism (on a quadruplet surface) because of a high activation barrier (~20000 K, which is much higher than the values recommended by various authors for the activation energy of this reaction, see Fig. 3). This reaction, which is the most important chain branching reaction (see calculations of the rate constants by a classical trajectory method in [40] and quantum calculations in [41] and references therein), mainly occurs by an indirect mechanism through the formation of the doublet intermediate complex $\{H\cdots O_2\}$, the vibrationally excited radical $HO_2(v)$. The lifetime of this intermediate complex (5×10^{-11} s according to an experimental study [42]) is comparable with the time between collisions. Consequently, the effect of particular experimental conditions through the vibrational relaxation process $HO_2(v) + M \longrightarrow HO_2(v-1) + M$ (see the results of calculations in Section 4) and chemical reactions with the participation of $HO_2(v)$ (see Section 3) should be considerable. We intend to perform a detailed kinetic calculation later on (taking into account various vibrational relaxation channels of the HO_2 radical) in terms of the mechanism

$$H + O_2 \longleftrightarrow HO_2(v)$$

and $\quad HO_2(v) + (M) \longleftrightarrow HO_2 + (M), \quad O + OH + (M),$

where (M) denotes the occurrence of the reaction both in the presence and in the absence of the third body M.

For comparison, reaction (5) (see the table) occurs on a triplet potential energy surface by a direct mechanism with a low activation energy. Reaction (26) (see the table) on a singlet surface occurs by an indirect mechanism via the formation of the intermediate complex $\{H_2\cdots O^*\}$, the vibrationally excited molecule of water (Fig. 4), and it is insignificant.

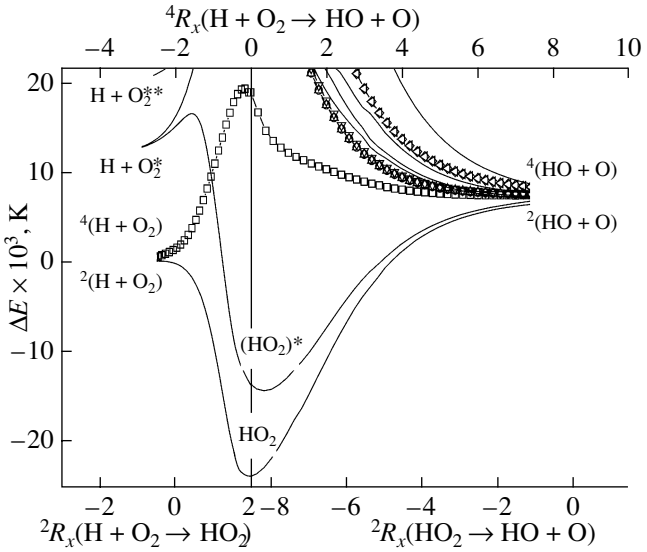

Fig. 3. Doublet and quadruplet (curves with markers) terms of the HO_2 system along the reaction paths from the states $H + O_2$, $H + O_2^*$, and $H + O_2^{**}$ to the states O + OH. The MCQDPT2 [25] energy profile along the CASSCF reaction coordinates R_x (the superscripts correspond to multiplicities). Full valence active space (13,9); 6–31** basis.

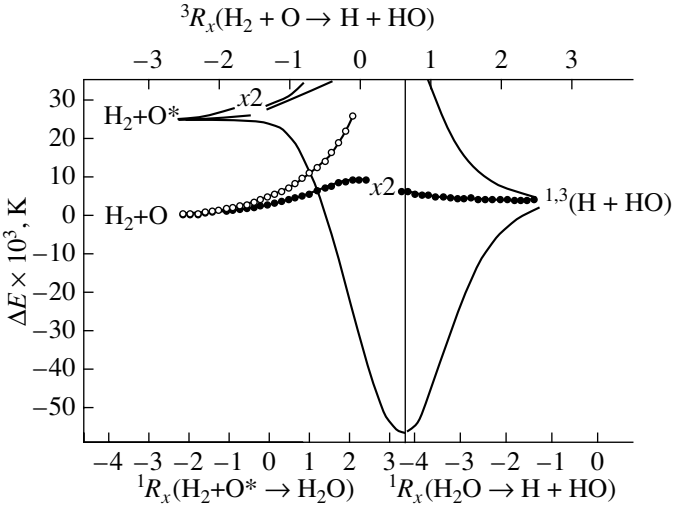

Fig. 4. Singlet and triplet (curves with markers) terms of the H_2O system along the reaction paths from the states $H_2 + O$ and $H_2 + O^*$ to the states H + OH. The MCQDPT2 [25] energy profile along the CASSCF reaction coordinates R_x (the superscripts correspond to multiplicities). Full valence active space (8,6); 6–31** basis.

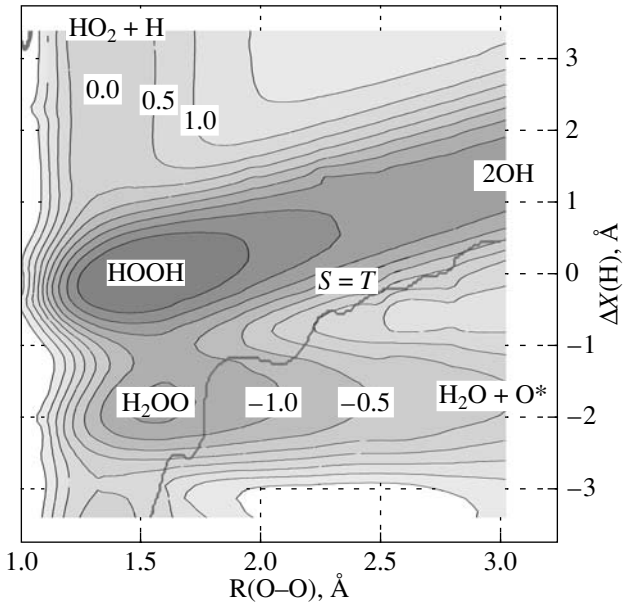

Fig. 5. Projection of the ground singlet term in the neighborhood of the potential well HOOH ⟷ H_2OO. R(O–O) is the distance between oxygen atoms; ΔX(H) is the shift of the H atom along the axis O–O. The other internal coordinates are fixed. $S = T$ is the line of intersection with the lower of three triplet terms of $H_2O + O$. The probability of spin-nonadiabatic predissociation into the channel $H_2O + O$ is negligibly small.

3. Reactions with the Participation of Electronically Excited Species

The increased apparent rate constants of reaction (4) (see the table) suggest the contribution of the reaction $H + O_2^* \longrightarrow O + OH$ (see Section 4). This is directly related to the participation of $HO_2(v)$ radicals in the regeneration of oxygen. Indeed, in accordance with experimental data [43], the rate constants of the processes $H + HO_2 \longrightarrow H_2 + O_2^*$ and $H + HO_2 \longrightarrow H_2 + O_2$ are in a ratio of 1 : 40 even at room temperature; this points clearly to the occurrence of considerable superequilibrium vibrational excitation of the HO_2 radical. According to our ab initio estimations, the difference between the activation energies of these reactions is 3500–5000 K, and the above ratio between the equilibrium rate constants of these processes is reached only at $T = 1000$–1500 K. The occurrence of secondary O_2^* molecules in an amount of 1% of O_2 will duplicate the rate of branching at $T = 1000$ K because the experimental rate constant of the reaction $H + O_2^* \longrightarrow HO + O$ [44] at $T = 1000$ K is higher than k_4^0 by two orders of magnitude.

The detailed mechanism of the formation of the electronically excited radical OH* is currently unknown. Process (16) (the table) is primarily responsible for the quantitative interpretation of our experiments [22] with the detection of OH*. The occurrence of the superequilibrium vibrational excitation of the radical HO_2=$HO_2(v)$ can increase the equilibrium rate constant of reaction (16) by several orders of magnitude. The bimolecular recombination $H + O_2 \longrightarrow HO_2(v)$, which occurs as a near-equilibrium process, serves as a source of the vibrationally excited radical $HO_2(v)$. This approach to the formation of the OH* radical is a detailed elaboration of the overall process $H + O_2 + H_2 \longrightarrow H_2O + OH^*$, which was proposed by Belles and Lauver [4] as early as 1964.

The O* atoms noticeably contribute to the formation of OH* by reaction (17). Because of this, attention was focused on the reaction $HO_2 + H \longrightarrow H_2O + O$, which has long since been assumed nonelementary (see [45] and references therein). The ab initio analysis of processes on the lower singlet sheet of the potential energy surface of the H_2O_2 system allowed us to ascribe the published rate constant of the reaction $HO_2 + H \longrightarrow H_2O + O$ to reaction (25), $HO_2 + H \longrightarrow H_2O + O^*$, followed by the quenching of O* atoms. Figure 5 shows a two-dimensional projection of the ground singlet term in the neighborhood of the intermediate complex, the joint potential well HOOH(v) ⟷ $H_2OO(v)$. The triplet surface (not shown) passes over the plane of the figure at the lower right of Fig. 5 ($H_2O + O$ channel). A classical trajectory method based on ab initio potentials, DRC from the GAMESS package, was used to evaluate the relative probability of degradation into $H_2O + O^*$ and 2HO channels. The (6,6)CASSCF/6–31** potential was minimally acceptable (the $H_2O + O^*$ outlet channel should lie lower than the $HO_2 + H$ inlet); the calculations were partially doubled using the

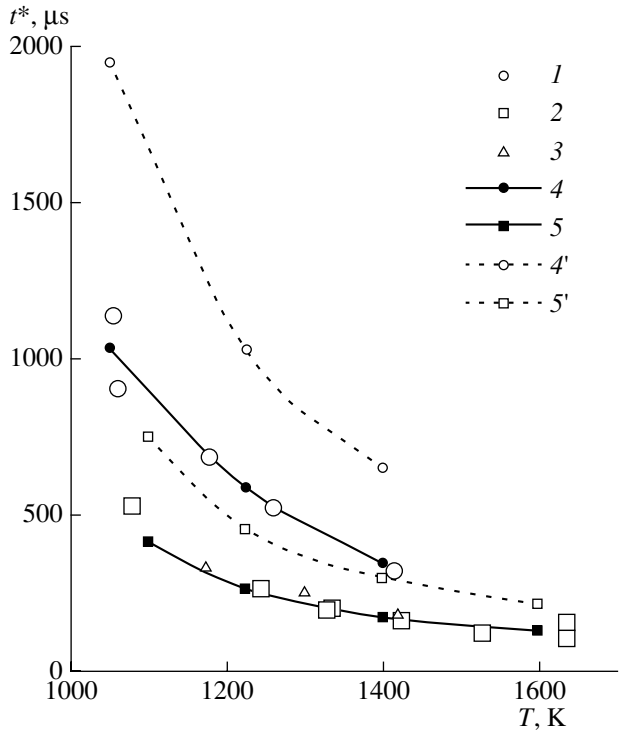

Fig. 6. Time between a shock front and the point in time at which luminescence reached a maximum (t^*) as a function of temperature (T) behind an incident shock wave: (*1–3*) experimental points obtained in stoichiometric ($H_2/O_2 = 2$; $\Phi = 1$) mixtures containing 1.4, 2.5, and 2.8% of a mixture of $2H_2 + O_2$ in Ar, respectively. The partial pressures of hydrogen were (8–37) × 10^{-3} atm. Calculations at (*4*, *5*) $k(H + O_2 \longrightarrow HO + O) = k^\wedge$ and (*4'*, *5'*) $k(H + O_2 \longrightarrow HO + O) = k_-$ (see Fig. 8).

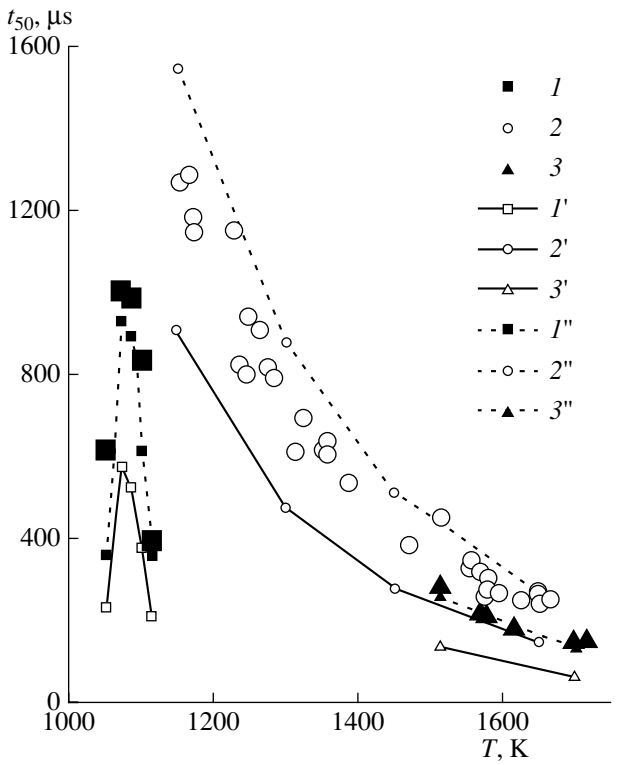

Fig. 7. Dependence of t_{50} (see Fig. 1) on temperature (T) behind a reflected shock wave (see the text): (*1–3*) experimental points [16] obtained in rich ($H_2/O_2 > 2$; $\Phi > 1$) mixtures. Partial pressures of hydrogen, atm: (*1*) (40–100) × 10^{-3}, (*2*) 16 × 10^{-3}, and (*3*) 80 × 10^{-3}. Calculations at (*1'–3'*) $k(H + O_2 \longrightarrow HO + O) = k^\wedge$ and (*1"–3"*) $k(H + O_2 \longrightarrow HO + O) = k_-$ (see Fig. 8).

(10,8)CASSCF/6–31** potential. At times to 10–15 vibrations along the O–H bond, about 30% returns to the $HO_2 + H$ channel were observed. The degradation of the complex at longer times is adequately described in terms of the Landau statistical theory. According to these estimations, the probability of the degradation $HO_2 + H \longrightarrow H_2O + O^*$ is ~10% of the probability of degradation into the main channel $HO_2 + H \longrightarrow 2HO$. The Landau–Zener probability of transition to the triplet channel $H_2O + O$ (spin-nonadiabatic predissociation) is negligibly small.

The ab initio heat of formation of HO_2, $\Delta H^f_{298}(HO_2) =$ 2.8 kcal/mol [26], which differs from the published value of 0.5 kcal/mol [36] and is within the limits of experimental error of more recent experimental results, 3.8 ± 1.2 [46] and 3.3 ± 0.8 kcal/mol [47], was used in the calculations.

4. Comparison between Calculated and Experimental Data and Conclusions

The experimental results [16, 22] were treated with the use of the kinetic scheme given in the table (Figs. 6, 7). Two series of calculations differed only in the apparent rate constants of process (4) $H + O_2 \longrightarrow O + OH$ k_- (lower value) and $k^\wedge$ (higher value) (Fig. 8, $k^\wedge/k_- \approx 2.5$–3). Note that many calculations performed with varying the rate constants of other reactions, either individually or in various combinations, within admissible limits did not furnish the desired result: a quantitative interpretation of the experimental data [16, 22] within the framework of a single kinetic scheme. The calculation with $k_4 = k^\wedge$ demonstrated very good agreement for experiments with the detection of electronically excited OH* (Fig. 6, low concentrations of H_2) and considerable inconsistency for experiments with the detection of OH radicals in the ground state (Fig. 7, high concentrations of H_2). The opposite situation was observed at $k_4 = k_-$.

Note that (see Fig. 8) the values of $k_4 = k^\wedge$ required for describing the experiments [22] are higher than the theoretically possible equilibrium values of $k_4^0 = (k_4^0)'K_{eq}$, which, in turn, cannot be higher than the values of k^0_{VTST} (the estimate of the equilibrium rate con-

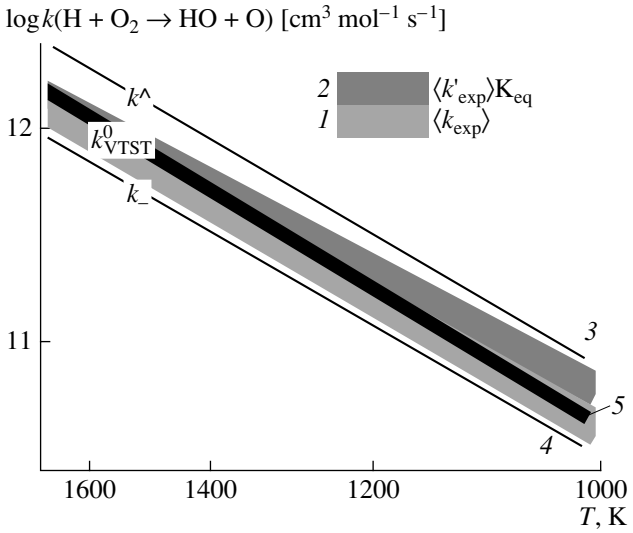

Fig. 8. Rate constant of the branching reaction $H + O_2 \longrightarrow HO + O$ according to various estimations: (*1*, *2*) averaged data (experimental only) [31] with consideration for the scatter of data $\langle k_{exp} \rangle = 9.1 \times 10^{13}\tau^{0.321}\exp(-8158/T)$ and $\langle k'_{exp} \rangle K_{eq} = 6.0 \times 10^{14}\tau^{-0.599}\exp(-8529/T)$; K_{eq} was taken from [36]; $\tau = T/298.15$. (*3*, *4*) Our estimates: $k^{\wedge} = 1.2 \times 10^{14}\tau^{0.5}\exp(-8000/T)$ and $k_{-} = 1.3 \times 10^{14} \times \exp(-8400/T)$, obtained by the kinetic treatment of experimental data (see the text). (*5*) $k^0_{VTST} = 5.4 \times 10^{14}\tau^{-0.266} \times \exp(-9184/T)$, found with the use of the (13,9)MCQDPT2/6–311+(3*df*,3*p*) potential curve and (13,9)CASSCF/6–311** frequencies (scale factors of 1.0538 and 1.024, respectively). The estimated accuracy is k^0_{VTST}, 10%.

stant by the transition state method is an upper estimate; for example, see [48]).

In conclusion, let us formulate the main results of this work and the main problems to be solved.

(1) The quantitative agreement/disagreement between calculation data and experimental results [16, 22] suggests the dependence of the apparent rate constant of the process $H + O_2 \longrightarrow O + OH$ on the concentration of the third body $M = H_2$. This is indicative of the inadequacy of equilibrium (Arrhenius) kinetics and the necessity of considering the most important overall chain-branching reaction $H + O_2 \longleftrightarrow HO_2(v) \longleftrightarrow O + OH$ with consideration for intramolecular energy redistribution in the $HO_2(v)$ radical and its vibrational relaxation in collisions. The development of a chain process is inhibited with the H_2 content supposedly because of the high efficiency of H_2 in the *VV'* deactivation of the high-frequency vibrational mode of $HO_2(v)$.

(2) The $HO_2(v)$ radical is the most important intermediate in the chain branching process and in the formation of the electronically excited species $O_2(^1\Delta)$ and $OH(^2\Sigma^+)$. This puts in the forefront the problem of a correct kinetic calculation of the superequilibrium vibrational excitation of HO_2 and its relaxation and indicates the direction of further studies, both experimental and theoretical. Thus, the availability of experimentally evaluated amounts of $O_2(^1\Delta)$ molecules in a mixture and the degrees of vibrational excitations of O_2 and $O_2(^1\Delta)$ molecules could provide the necessary control points for calculations performed with consideration for nonequilibrium.

(3) The new mechanisms of formation and quenching of electronically excited $OH(^2\Sigma^+)$ radicals, $O(^1D)$ atoms, and $O_2(^1\Delta)$ molecules in the course of combustion are proposed; they are of importance for interpreting experiments performed using emission spectroscopy.

ACKNOWLEDGMENTS

This work was supported by the Russian Foundation for Basic Research (project no. 04-03-32678), the Presidium of the Russian Academy of Sciences (OKhNM Basic Research Program no. 1; coordinator: O.M. Nefedov), and INTAS (grant no. 03-51-4736).

REFERENCES

1. Semenov, N.N., *Tsepnye reaktsii* (Chain Reactions), Leningrad: Goskhimtekhizdat, 1934.
2. Semenov, N.N., *O nekotorykh problemakh khimicheskoi kinetiki i reaktsionnoi sposobnosti* (Some Problems of Chemical Kinetics and Reactivity), Moscow: Akad. Nauk SSSR, 1958.
3. Lewis, B. and von Elbe, G., *Combustion, Flames, and Explosions of Gases*, New York: Academic, 1961.
4. Belles, F.E. and Lauver, M.R., *J. Chem. Phys.*, 1964, vol. 40, p. 415.
5. Ripley, D.L. and Gardner, W.C., *J. Chem. Phys.*, 1966, vol. 44, p. 2285.
6. Safaryan, M.N., Skrebkov, O.V., Vasil'ev, V.M., and Stesik, L.N., *Rep. no. 1529 of the Branch of the Inst. of Chemical Physics*, Chernogolovka, Moscow oblast, 1967.
7. Kondratiev, V.N., in *Comprehensive Chemical Kinetics*, Amsterdam: Elsevier, 1969, vol. 2, p. 119.
8. Jachimowski, C.J. and Houghton, W.M., *Combust. Flame*, 1971, vol. 17, p. 25.
9. Kondrat'ev, V.N. and Nikitin, E.E., *Kinetika i mekhanizm gazofaznykh reaktsii* (Kinetics and Mechanism of Gas-Phase Reactions), Moscow: Nauka, 1974.
10. Schott, G.L. and Getzinger, R.W., in *Physical Chemistry of Fast Reactions*, vol. 1: *Gas Phase Reactions of Small Molecules*, London: Plenum, 1973.
11. Dougherty, E.P., Rabitz. H, *J. Chem. Phys.*, 1980, vol. 72, p. 6571.
12. Kondrat'ev, V.N. and Nikitin, E.E., *Khimicheskie protsessy v gazakh* (Chemical Processes in Gases), Moscow: Nauka, 1981.
13. Maas, U. and Warnatz, J., *Combust. Flame*, 1988, vol. 74, p. 53.

14. Maas, U. and Pope, S.B., *Combust. Flame*, 1992, vol. 88, p. 239.
15. Tonello, N.A., Sichel, M., and Oran, E.S., *15th ICDERS*, Colorado, 1995, p. 51.
16. Ryu, S.O., Hwang, S.M., and Rabinovitz, M.J., *J. Phys. Chem.*, 1995, vol. 99, p. 13 984.
17. Blumenthal, R., Fieweger, K., Komp, K.H., et al., *20th Int. Symp. on Shock Tubes and Waves*, Pasadena, 1996, p. 935.
18. Azatyan, V.V. and Merzhanov, A.G., *Khimicheskaya fizika na poroge XXI veka* (Chemical Physics at the Turn of the 21st Century), Moscow: Nauka, 1996.
19. Divakov, O.G., Eremin, A.V., Ziborov, V.S., and Fortov, V.E., *Dokl. Akad. Nauk*, 2000, vol. 373, no. 4, p. 487 [*Dokl. Chem.* (Engl. Transl.), vol. 373, nos. 4–6, p. 141].
20. Michael, J.V., Suhterland, J.W., Harding, L.B., and Wagner, A.F., *Proc. Combust. Inst.*, 2000, vol. 28, p. 1471.
21. Starik, A.M. and Titova, N.S., *Khim. Fiz.*, 2001, vol. 20, no. 5, p. 17.
22. Skrebkov, O.V., Myagkov, Yu.P., Karkach, S.P., et al., *Dokl. Akad. Nauk*, 2002, vol. 383, no. 6, p. 1 [*Dokl. Phys. Chem.* (Engl. Transl.), vol. 383, nos. 4–6, p. 93].
23. Skrebkov, O.V., Karkach, S.P., Vasil'ev, V.M., and Smirnov, A.L., *Chem. Phys. Lett.*, 2003, vol. 375, p. 413.
24. Frisch, M.J., Trucks, G.W., Schlegel, H.B., et al., *Gaussian-94, Revision C.4*, Pittsburg, PA: Gaussian Inc., 1995.
25. Schmidt, M.W., Baldridge, K.K., Boatz, J.A., et al., *J. Comput. Chem.*, 1993, vol. 14, p. 1347.
26. Karkach, S.P. and Osherov, V.I., *J. Chem. Phys.*, 1999, vol. 110, p. 11918.
27. Nikitin, E.E., *Teoriya elementarnykh atomno-molekulyarnykh protsessov v gazakh* (Theory of Elementary Atomic and Molecular Processes in Gases), Moscow: Khimiya, 1970.
28. Vasil'ev, V.M., Kulikov, S.V., and Skrebkov, O.V., *Prikl. Mekh. Tekh. Fiz.*, 1977, vol. 13.
29. Skrebkov, O.V. and Kulikov, S.V., *Chem. Phys.*, 1998, vol. 227, p. 349.
30. Baulch, D.L., Cobos, C.J., Cox, R.A., et al., *Combust. Flame*, 1994, vol. 98, p. 59.
31. Mallard, W.G., Westley, F., Herron, J.T., and Hampson, R.F., *NIST Chemical Kinetics Database, Ver. 6.0*, Gaithersburg, Md., 1994.
32. Fairchild, P.W., Smith, G.P., and Crosley, D.R., *J. Chem. Phys.*, 1983, vol. 79, p. 1795.
33. Smith, G.P. and Crosley, D.R., *J. Chem. Phys.*, 1986, vol. 85, p. 3896.
34. Carrington, T., *J. Chem. Phys.*, 1959, vol. 30, p. 1087.
35. Huber, K.-P. and Herzberg, G., *Molecular Spectra and Molecular Structure*, New York: van Nostrand, 1979.
36. 37. Filatov, M., Reckien, W., Peyerimhoff, S.D., and Shaik, S., *J. Phys. Chem. A*, 2000, vol. 104, p. 12014.
38. Volokhov, V.M., Voronin, A.I., Karkach, S.P., et al., *Khim. Fiz.*, 1998, vol. 17, no. 8, p. 3.
39. Karkach, S.P., Osherov, V.I., and Ushakov, V.G., *Khim. Fiz.*, 2000, vol. 19, no. 10, p. 3.
40. Miller, J.A., *J. Chem. Phys.*, 1981, vol. 74, p. 5120.
41. Lin, S.Y., Rackham, E.J., and Guo, H., *J. Phys. Chem. A*, 2006, vol. 110, p. 1534.
42. Wadlinger, R.L. and Darwent, B. de B., *J. Phys. Chem.*, 1967, vol. 71, p. 2057.
43. Washida, N., Akimoto, H., and Okuda, M., *J. Phys. Chem.*, 1978, vol. 82, p. 18.
44. Basevich, V.Ya. and Vedeneev, V.I., *Khim. Fiz.*, 1985, vol. 4, no. 8, p. 1102.
45. Shaw, R., *Int. J. Chem. Kinet.*, 1977, vol. 9, p. 929.
46. Fisher, E.R. and Armentrout, P.B., *J. Phys. Chem.*, 1990, vol. 94, p. 4396.
47. Litorja, M. and Ruscic, B., *J. Electron Spectrosc. Relat. Phenom.*, 1998, vol. 97, p. 131.
48. Kondrat'ev, V.N., Nikitin, E.E., Reznikov, A.I., and Umanskii, S.Ya., *Termicheskie bimolekulyarnye reaktsii v gazakh* (Thermal Bimolecular Reactions in Gases), Moscow: Nauka, 1976.